

On Time Fractional Modified Camassa-Holm and Degasperis-Procesi Equations by Using the Haar Wavelet Iteration Method

N. Aghazadeh, Gh. Ahmadnezhad, Sh. Rezapour*

Department of Mathematics, Azarbaijan Shahid Madani University, Tabriz,
Iran

E-mail: aghazadeh@azaruniv.ac.ir
E-mail: hazharahmadnezhad@gmail.com
E-mail: sh.rezapour@azaruniv.ac.ir

ABSTRACT. The Haar wavelet collocation with iteration technique is applied for solving a class of time-fractional physical equations. The approximate solutions obtained by two dimensional Haar wavelet with iteration technique are compared with those obtained by analytical methods such as Adomian decomposition method (ADM) and variational iteration method (VIM). The results show that the present scheme is effective and appropriate for obtaining the numerical solution of the time-fractional Modified Camassa-Holm equation and Time fractional Modified Degasperis-Procesi equation.

Keywords: Fractional differential equation, Haar wavelet, Operational matrices, Iterative method, Sylvester equation.

2000 Mathematics subject classification: 26A33, 45K05, 65T60.

1. INTRODUCTION

Many phenomena in various fields of the science and engineering can be modeled by fractional differential equations. The applications of fractional

*Corresponding Author

calculus have been demonstrated by many authors. For examples, fractional calculus is applied to model the nonlinear oscillation of earthquake [1], fluid-dynamic traffic [2], continuum and statistical mechanics [3], signal processing [4], control theory [5], and dynamics of interfaces between nanoparticles and substrates [6].

Recently, orthogonal wavelets bases are becoming more popular for numerical solutions of partial differential equations due to their excellent properties such as ability to detect singularities, orthogonality, flexibility to represent a function at different levels of resolution, and compact support. In recent years, there has been a growing interest in developing wavelet based on numerical algorithms for solution of fractional order partial differential equations ([7-15]). Among them, the Haar wavelet method is the simplest and easiest to use. Haar wavelets have been successfully applied for the solutions of ordinary and partial differential equations, integral equations, and integro-differential equations.

In this work, we solve a family of important physically equations by combining Haar wavelet method and an iteration technique. We describe the nonlinear fractional partial differential equation by an iteration technique and then convert the obtained discretized equation into a Sylvester equation by the Haar wavelet method to get the solution.

The above mentioned partial differential equation is as follows:

$$u_t^\alpha - u_{xxt} + (b+1)u^2u_x = bu_xu_{xx} + uu_{xxx}, \quad (1.1)$$

with the initial and boundary conditions:

$$u(x, 0) = g(x), \quad u(0, t) = y_0(t), \quad u(1, t) = y_1(t), \quad t \geq 0, \quad 0 < x < 1,$$

where b is a positive integer. For $b = 2$ and $b = 3$ Eq. (1.1) reduces to Time Fractional Modified Camassa-Holm equation and Time Fractional Modified Degasperis-Procesi equation, respectively.

The Camassa-Holm equation is used to describe physical model for the uni-directional propagation of waves in shallow water [19, 20]. This equation is widely used in fluid dynamics, continuum mechanics, aerodynamics, and models for shock wave formation, solitons, turbulence, mass transport, and the solution representing the waters free surface above a flat bottom [21, 22]. The Camassa-Holm equation has been obtained by Fokas and Fuchssteiner [23] and Lenells [24]. Camassa and Holm [25] put forward the derivation of the solution as a model for dispersive shallow water waves and revealed that it is formally integrable finite dimensional Hamiltonian system and its solitary waves are solitons. Many analytical methods have been implemented in recent past for the study of nonlinear fractional differential equations arising in mathematical physics [26-35]. Note that, there are some new papers on the time-fractional diffusion equation in signal processing (see for example, [36] and [37]). The Degasperis-Procesi equation was discovered by Degasperis and Procesi in a

search for integrable equations similar in form to the Camassa-Holm equation, and is widely used in fluid dynamics, aerodynamics, optimal fiber, biology, solid state physics, geometry and oceanology.

2. HAAR WAVELET AND OPERATIONAL MATRIX OF GENERAL ORDER INTEGRATION

The i th uniform Haar wavelet $h_i(x)$, $x \in [0, 1]$ is defined as:

$$h_i(x) = \begin{cases} 1 & a(i) \leq x \leq b(i) \\ -1 & b(i) \leq x < c(i) \\ 0 & otherwise \end{cases} \quad (2.1)$$

where $a(i) = \frac{k-1}{m}$, $b(i) = \frac{k-0.5}{m}$, $c(i) = \frac{k}{m}$, $i = 2^j + k + 1$, $j = 0, 1, 2, 3, \dots, J$ is dilation parameter, $m = 2^{p+1}$ and $k = 0, 1, 2, \dots, 2^j - 1$ is translation parameter. The Maximum level of resolution is J . In particular $h_1(x) = \chi_{[0,1)}(x)$, where $\chi_{[0,1)}(x)$ is characteristic function on interval $[0,1)$, is the Haar scaling function. Let us define the collocation points $x_j = \frac{j-0.5}{m}$ where $j = 1, 2, 3, \dots, m$.

We establish an operational matrix for integration via Haar wavelets. The operational matrix of integration of general order is obtained by integration Eq. (2.1) is as follows:

$$\begin{aligned} P_{\alpha,1}(x) &= I_{a(1)}^\alpha h_1(x) \\ &= \frac{1}{\Gamma(\alpha)} \int_{a(1)}^x (x-s)^{\alpha-1} ds, \quad \alpha > 0. \end{aligned} \quad (2.2)$$

$$\begin{aligned} P_{\alpha,i}(x) &= I_a^\alpha h_i(x) = \frac{1}{\Gamma(\alpha)} \\ &\begin{cases} \int_{a(i)}^x (x-s)^{\alpha-1} ds & a(i) \leq x < b(i), \\ \int_{a(i)}^{b(i)} (x-s)^{\alpha-1} ds - \int_{b(i)}^x (x-s)^{\alpha-1} ds & b(i) \leq x < c(i), \\ \int_{a(i)}^{b(i)} (x-s)^{\alpha-1} ds - \int_{b(i)}^{c(i)} (x-s)^{\alpha-1} ds & x \geq c(i). \end{cases} \end{aligned} \quad (2.3)$$

By simplifying:

$$P_{\alpha,1}(x) = \frac{(x-a(1))^\alpha}{\Gamma(\alpha+1)}, \quad (2.4)$$

and

$$\begin{aligned} P_{\alpha,i}(x) &= I_a^\alpha h_i(x) = \frac{1}{\Gamma(\alpha+1)} \\ &\begin{cases} (x-a(i))^\alpha & a(i) \leq x < b(i), \\ (x-a(i))^\alpha - 2(x-b(i))^\alpha & b(i) \leq x < c(i), \\ (x-a(i))^\alpha - 2(x-b(i))^\alpha + (x-c(i))^\alpha & x \geq c(i). \end{cases} \end{aligned} \quad (2.5)$$

Any function $y \in L^2[0, 1]$ can be expressed in terms of the Haar wavelet as:

$$y(x) = \sum_{i=1}^{\infty} c_i h_i(x), \quad (2.6)$$

where c_i s are the Haar wavelet coefficients given by $c_i = \int_0^1 y(x)h_i(x)dx$.

We can approximate the function $y(x)$ by the truncated series

$$y(x) \approx \sum_{i=1}^{m-1} c_i h_i(x). \quad (2.7)$$

Taking the collocation point as $x(i) = \frac{i-0.5}{m}$ where $i = 1, 2, \dots, m$ we define Haar wavelet matrix $H_{m \times m}$ as:

$$H_{m \times m} = \begin{pmatrix} h_1(x(1)) & h_1(x(2)) & \cdots & h_1(x(m)) \\ h_2(x(1)) & h_2(x(2)) & \cdots & h_2(x(m)) \\ \vdots & \vdots & \ddots & \vdots \\ h_m(x(1)) & h_m(x(2)) & \cdots & h_m(x(m)) \end{pmatrix}.$$

We can represent equation (2.7) in vector form as $y = cH$ where $c = [c_1, c_2, \dots, c_m]$. The Haar coefficient c_i can be evaluated by $c = yH^{-1}$ where H^{-1} is inverse of H . Similarly we can obtain the fractional order integration matrix P of Haar function by substituting the collocation points in Eqs. (2.4) and (2.5).

$$P_{m \times m}^\alpha = \begin{pmatrix} P_{\alpha,1}(x(1)) & P_{\alpha,1}(x(2)) & \cdots & P_{\alpha,1}(x(m)) \\ P_{\alpha,2}(x(1)) & P_{\alpha,2}(x(2)) & \cdots & P_{\alpha,2}(x(m)) \\ \vdots & \vdots & \ddots & \vdots \\ P_{\alpha,m}(x(1)) & P_{\alpha,m}(x(2)) & \cdots & P_{\alpha,m}(x(m)) \end{pmatrix}.$$

For example if $m = 8$, $\alpha = 0.9$, the Haar wavelet matrix of fractional integration is:

$$P_{8 \times 8}^{0.9} = \begin{pmatrix} 0.0857 & 0.2305 & 0.3650 & 0.4941 & 0.6195 & 0.7421 & 0.8625 & 0.9811 \\ 0.0857 & 0.2305 & 0.3650 & 0.4941 & 0.4480 & 0.2812 & 0.1325 & -0.0071 \\ 0.0857 & 0.2305 & 0.1935 & 0.0331 & -0.0248 & -0.156 & -0.115 & -0.0091 \\ 0 & 0 & 0 & 0 & 0.0857 & 0.2305 & 0.1935 & 0.0331 \\ 0.0857 & 0.0590 & -0.0102 & -0.0054 & -0.0037 & -0.0028 & -0.0022 & -0.0018 \\ 0 & 0 & 0.0857 & 0.0590 & -0.0102 & -0.0054 & -0.0037 & -0.0028 \\ 0 & 0 & 0 & 0 & 0.0857 & 0.0590 & -0.0102 & -0.0054 \\ 0 & 0 & 0 & 0 & 0 & 0 & 0.0857 & 0.0590 \end{pmatrix}.$$

We derive another operational matrix of fractional integration to solve the fractional boundary value problems. Let $\eta > 0$ and $g : [0, \eta] \rightarrow \mathbb{R}$ be a continuous function and assume that Haar function have $[0, \eta)$ as compact support, then

$$g(x)I_0^\alpha h_1(\eta) = g(x) \int_0^\eta (\eta - s)^{\alpha-1} ds \quad (2.8)$$

$$v^{\alpha, \eta, 1} = g(x)C_{\alpha, 1}$$

and

$$g(x)I_0^\alpha h_i(\eta) = g(x) \left\{ \int_{a(i)}^{b(i)} (\eta - s)^{\alpha-1} ds - \int_{b(i)}^{c(i)} (\eta - s)^{\alpha-1} ds \right\} \quad (2.9)$$

$$v^{\alpha, \eta, i} = g(x)C_{\alpha, i}$$

where $C_{\alpha, 1} = \frac{\eta^\alpha}{\Gamma(\alpha+1)}$, $C_{\alpha, i} = \frac{1}{\Gamma(\alpha+1)} \left[(\eta - a(i))^\alpha - 2(\eta - b(i))^\alpha + (\eta - c(i))^\alpha \right]$.

By using the collocation points, we get:

$$V_{m \times m}^{\alpha, \eta, g(x)} = \begin{pmatrix} g(x(1))I_0^\alpha h_1(\eta) & g(x(2))I_0^\alpha h_1(\eta) & \cdots & g(x(m))I_0^\alpha h_1(\eta) \\ g(x(1))I_0^\alpha h_2(\eta) & g(x(2))I_0^\alpha h_2(\eta) & \cdots & g(x(m))I_0^\alpha h_2(\eta) \\ \vdots & \vdots & \ddots & \vdots \\ g(x(1))I_0^\alpha h_m(\eta) & g(x(2))I_0^\alpha h_m(\eta) & \cdots & g(x(m))I_0^\alpha h_m(\eta) \end{pmatrix}.$$

In particular, for $\eta = 1$, $g(x) = x$, $\alpha = 0.9$, $m = 8$, we get:

$$V_{8 \times 8}^{0.9, 1, x} = \begin{pmatrix} .0650 & .1950 & .3249 & .4549 & .5849 & .7148 & .8448 & .9748 \\ -.0047 & -.0140 & -.0233 & -.0326 & -.0420 & -.0513 & -.0606 & -.0700 \\ -.0005 & -.0015 & -.0026 & -.0036 & -.0046 & -.0056 & -.0067 & -.0077 \\ -.0025 & -.0075 & -.0125 & -.0175 & -.0225 & -.0275 & -.0325 & -.0375 \\ -.0001 & -.0003 & -.0005 & -.0007 & -.0009 & -.0012 & -.0014 & -.0016 \\ -.0001 & -.0004 & -.0007 & -.0011 & -.0014 & -.0017 & -.0020 & -.0023 \\ -.0002 & -.0008 & -.0014 & -.0019 & -.0025 & -.0030 & -.0036 & -.0041 \\ -.0013 & -.0040 & -.0067 & -.0094 & -.0121 & -.0147 & -.0174 & -.0201 \end{pmatrix}.$$

3. CONVERGENCE

Theorem 3.1. Suppose that the functions $u_m(x, t)$ obtained by using Haar wavelet are the approximation of $u(x, t)$, then we have the following error bound:

$$\|u(x, t) - u_m(x, t)\|_E \leq \frac{K}{\sqrt{3m}}$$

$$\|u(x, t)\|_E = \left(\int_0^1 \int_0^1 u^2(x, t) dx dt \right)^{1/2}. \quad (3.1)$$

Proof. Suppose $u_m(x, t)$ is the following approximation of $u(x, t)$,

$$u_m(x, t) = \sum_{n=0}^{m-1} \sum_{l=0}^{m-1} u_{nl} h_n(x) h_l(t).$$

Then we have:

$$u(x, t) - u_m(x, t) = \sum_{n=m}^{\infty} \sum_{l=m}^{\infty} u_{nl} h_n(x) h_l(t) = \sum_{n=2^{p+1}}^{\infty} \sum_{l=2^{p+1}}^{\infty} u_{nl} h_n(x) h_l(t).$$

The orthogonality of the sequence $h_i(x)$ on $[0, 1)$ implies that

$$h_l(\cdot) = 2^{\frac{j}{2}} h(2^j(\cdot) - k). \quad (3.2)$$

Therefore

$$\begin{aligned}
\|u(x, t) - u_m(x, t)\|_E^2 &= \int_0^1 \int_0^1 (u(x, t) - u_m(x, t))^2 dx dt \\
&= 2^j \sum_{n=2^{p+1}}^{\infty} \sum_{l=2^{p+1}}^{\infty} \sum_{n'=2^{p+1}}^{\infty} \sum_{l'=2^{p+1}}^{\infty} u_{nl} u_{n'l'} \quad (3.3) \\
&\quad \left(\int_0^1 h_n(x) h_{n'}(x) dx \right) \left(\int_0^1 h_l(t) h_{l'}(t) dt \right) \\
&= 2^j \sum_{n=2^{p+1}}^{\infty} \sum_{l=2^{p+1}}^{\infty} u_{nl}^2, \quad (3.4)
\end{aligned}$$

where $u_{nl} = \langle h_n(x), \langle u(x, t), h_l(t) \rangle \rangle$.

According to Eq. (2.1) and the inner product definition, we have:

$$\begin{aligned}
\langle u(x, t), h_l(t) \rangle &= \int_0^1 u(x, t) h_l(t) dt \\
&= 2^{\frac{j}{2}} \left(\int_{\frac{k-1}{2^j}}^{\frac{k-0.5}{2^j}} u(x, t) dt - \int_{\frac{k-0.5}{2^j}}^{\frac{k}{2^j}} u(x, t) dt \right). \quad (3.5)
\end{aligned}$$

By using mean value theorem of integrals:

$$\exists t_1, t_2 : \quad \frac{k-1}{2^j} \leq t_1 < \frac{k-0.5}{2^j}, \quad \frac{k-0.5}{2^j} \leq t_2 < \frac{k}{2^j}, \quad (3.6)$$

so that

$$\begin{aligned}
\langle u(x, t), h_l(t) \rangle &= 2^{\frac{j}{2}} \left(\left(\frac{k-0.5}{2^j} - \frac{k-1}{2^j} \right) u(x, t_1) - \left(\frac{k}{2^j} - \frac{k-0.5}{2^j} \right) u(x, t_2) \right) \\
&= \frac{2^{\frac{j}{2}}}{2^{j+1}} \left(u(x, t_1) - u(x, t_2) \right) \quad (3.7)
\end{aligned}$$

$$u_{nl} = \left\langle h_n(x), \frac{1}{2^{\frac{j}{2}+1}} (u(x, t_1) - u(x, t_2)) \right\rangle \quad (3.8)$$

$$\begin{aligned}
&= \frac{1}{2^{j+1}} \int_0^1 h_n(x) (u(x, t_1) - u(x, t_2)) dx \\
&= \frac{2^{\frac{j}{2}}}{2^{\frac{j}{2}+1}} \left(\int_{\frac{k-1}{2^j}}^{\frac{k-0.5}{2^j}} u(x, t_1) dx - \int_{\frac{k-0.5}{2^j}}^{\frac{k}{2^j}} u(x, t_1) dx \right. \\
&\quad \left. - \int_{\frac{k-1}{2^j}}^{\frac{k-0.5}{2^j}} u(x, t_2) dx + \int_{\frac{k-0.5}{2^j}}^{\frac{k}{2^j}} u(x, t_2) dx \right). \quad (3.9)
\end{aligned}$$

(3.10)

By using mean value theorem of integrals again we have:

$$\exists x_1, x_2, x_3, x_4 : \quad \frac{k-1}{2^j} \leq x_1, x_2 < \frac{k-0.5}{2^j}, \quad \frac{k-0.5}{2^j} \leq x_3, x_4 < \frac{k}{2^j}$$

$$\begin{aligned}
u_{nl} &= \frac{1}{2} \left\{ \left(\frac{k-0.5}{2^j} - \frac{k-1}{2^j} \right) u(x_1, t_1) - \left(\frac{k}{2^j} - \frac{k-0.5}{2^j} \right) u(x_2, t_1) - \right. \\
&\quad \left. \left(\frac{k-0.5}{2^j} - \frac{k-1}{2^j} \right) u(x_3, t_2) + \left(\frac{k}{2^j} - \frac{k-0.5}{2^j} \right) u(x_4, t_2) \right\} \\
&= \frac{1}{2^{j+2}} \left\{ (u(x_1, t_1) - u(x_2, t_1)) - (u(x_3, t_2) - u(x_4, t_2)) \right\} \quad (3.11)
\end{aligned}$$

$$u_{nl}^2 = \frac{1}{2^{2j+4}} \left\{ (u(x_1, t_1) - u(x_2, t_1)) - (u(x_3, t_2) - u(x_4, t_2)) \right\}^2.$$

By using mean value theorem of derivatives:

$$\exists \xi_1, \xi_2 : x_1 \leq \xi_1 < x_2, \quad x_3 \leq \xi_2 < x_4$$

so that

$$\begin{aligned}
u_{nl}^2 &\leq \frac{1}{2^{2j+4}} \left\{ (x_2 - x_1)^2 \left[\frac{\partial u(\xi_1, t_1)}{\partial x} \right]^2 + (x_4 - x_3)^2 \left[\frac{\partial u(\xi_2, t_2)}{\partial x} \right]^2 \right. \\
&\quad \left. + 2(x_2 - x_1)(x_4 - x_3) \left| \frac{\partial u(\xi_1, t_1)}{\partial x} \right| \left| \frac{\partial u(\xi_2, t_2)}{\partial x} \right| \right\}. \quad (3.12)
\end{aligned}$$

We assume that $\frac{\partial u(x, t)}{\partial x}$ is continuous and bounded on $(0, 1) \times (0, 1)$, then

$$\exists K > 0, \forall x, t \in (0, 1) \times (0, 1), \quad \left| \frac{\partial u(x, t)}{\partial x} \right| \leq K. \quad (3.13)$$

$$u_{nl}^2 \leq \left(\frac{1}{2^{2j+4}} \right) \frac{4K^2}{2^{2j}} = \frac{4K^2}{2^{4j+4}}. \quad (3.14)$$

By substituting Eq. (3.14) into Eq. (3.3), we have

$$\begin{aligned}
\|u(x, t) - u_m(x, t)\|_E^2 &= \sum_{j=p+1}^{\infty} \left(\sum_{n=2^j}^{2^{j+1}-1} \sum_{n=2^j}^{2^{j+1}-1} u_{nl}^2 \right) \\
&\leq \sum_{j=p+1}^{\infty} \left(\sum_{n=2^j}^{2^{j+1}-1} \sum_{n=2^j}^{2^{j+1}-1} \frac{4K^2}{2^{4j+4}} \right) \\
&= 4K^2 \sum_{j=p+1}^{\infty} \left(\sum_{n=2^j}^{2^{j+1}-1} \sum_{n=2^j}^{2^{j+1}-1} \frac{1}{2^{4j+4}} \right) \\
&= \frac{K^2}{3} \frac{1}{4^{p+1}} = \frac{K^2}{3m^2}. \quad (3.15)
\end{aligned}$$

Therefore

$$\|u(x, t) - u_m(x, t)\|_E \leq \frac{K}{\sqrt{3m}}. \quad (3.16)$$

From the Eq. (3.16), we can find that $\|u(x, t) - u_m(x, t)\|_E \rightarrow 0$ when $m \rightarrow \infty$. The larger the value of m , the more accurate the numerical solution. with similar procedure, we have

$$\|u_{r+1}(x, t) - u_{r+1}^m(x, t)\|_E \leq \frac{K}{\sqrt{3m}}. \quad (3.17)$$

Eq. (3.17) implies that error between the exact and approximate solution at the $(r+1)$ th iteration is inversely proportional to the maximal level of resolution. This implies that $u_{r+1}^m(x, t)$ converges to $u_{r+1}(x, t)$ as $m \rightarrow \infty$. Since $u_{r+1}(x, t)$ is obtained at $(r+1)$ th iteration of Picard technique then according to the convergence analysis of Picard technique which states that $u_{r+1}(x, t)$ converges to $u(x, t)$ as r approaches to infinity. This suggests that solution by Haar wavelet Picard technique, $u_{r+1}^m(x, t)$, converges to $u(x, t)$ as m and r approaches to infinity. \square

4. DESCRIPTION OF THE PROPOSED METHOD

By applying the iteration method (Picard iteration) to Eq. (1.1), we get

$$\frac{\partial^\alpha u_{r+1}}{\partial t^\alpha} - \frac{\partial^3 u_{r+1}}{\partial x^2 \partial t} = -(b+1)u_r^2 \frac{\partial u_r}{\partial x} + b \frac{\partial u_r}{\partial x} \frac{\partial^2 u_r}{\partial x^2} + u_r \frac{\partial^3 u_r}{\partial x^3} \quad (4.1)$$

for $0 < \alpha \leq 1$, $b > 0$, with the initial and boundary condition:

$$u_{r+1}(x, 0) = g(x), \quad u_{r+1}(0, t) = y_0(t), \quad u_{r+1}(1, t) = y_1(t),$$

with $t \geq 0$, $0 < x < 1$.

By applying the Haar wavelet method, we suppose:

$$\frac{\partial^3 u_{r+1}}{\partial x^2 \partial t} = \sum_{i=1}^{2M} \sum_{j=1}^{2M} C_{i,j}^{r+1} h_i(x) h_j(t) = H^T(x) C^{r+1} H(t). \quad (4.2)$$

By applying the integral operator I_x^2 on Eq. (4.2):

$$\frac{\partial u_{r+1}}{\partial t} = (P_x^2)^T C^{r+1} H(t) + p(t)x + q(t). \quad (4.3)$$

By using the boundary condition and put $x = 0$, $x = 1$, we get:

$$\begin{aligned} x = 0 & : \quad q(t) = \frac{\partial y_0}{\partial t} \\ x = 1 & : \quad p(t) = \frac{\partial y_1}{\partial t} - \frac{\partial y_0}{\partial t} - (P_x^2(1))^T C^{r+1} H(t). \end{aligned}$$

By applying the integral operator I_t^1 to Eq. (4.3) :

$$u_{r+1}(x, t) = (P_x^2)^T C^{r+1} P_t + x \left\{ y_1(t) - y_0(t) - (P_x^2(1))^T C^{r+1} P_t \right\} + y_0(t) + r(x), \quad (4.2)$$

we use the initial condition and put $t = 0$ to get:

$$t = 0 : \quad r(x) = g(x) - x \{ y_1(0) - y_0(0) \} - y_0(0).$$

By derivating from Eq. (4.2), we get:

$$\frac{\partial u_r}{\partial x} = (P_x)^T C^{r+1} P_t + \left(y_1(t) - y_0(t) - (P_x^2(1))^T C^{r+1} P_t \right) + \frac{\partial r(x)}{\partial x}, \quad (4.2)$$

$$\frac{\partial^2 u}{\partial x^2} = H^T(x) C^{r+1} P_t + \frac{\partial^2 r(x)}{\partial x^2}. \quad (4.3)$$

We estimate right side or nonlinear part of Eq. (4.1) by Haar wavelet:

$$\begin{aligned} S(x, t) &= b \frac{\partial u_r}{\partial x} \frac{\partial^2 u_r}{\partial x^2} - (b+1) u_r^2 \frac{\partial^2 u_r}{\partial x^2} + u_r \frac{\partial u_r^3}{\partial x^3} \\ &= \sum_{i=1}^{2M} \sum_{j=1}^{2M} m_{i,j} h_i(x) h_j(t) \\ &= H^T(x) M H(t), \end{aligned} \quad (4.3)$$

where $m_{i,j} = \langle h_i(x), \langle S(x, t), h_j(t) \rangle \rangle$. By substituting Eqs. (4.4) and (4.2) for Eq. (4.1), we get:

$$\frac{\partial^\alpha u_{r+1}}{\partial t^\alpha} = H^T(x) C^{r+1} H(t) + H^T(x) M H(t). \quad (4.3)$$

By applying fractional integral operator I_t^α to Eq. (4.3) and using the initial conditions, we obtain:

$$u_{r+1}(x, t) = H^T(x) C^{r+1} P_t^\alpha + H^T(x) M P_t^\alpha + g(x). \quad (4.4)$$

From Eqs. (4.4) and (4.2), we get:

$$K(x, t) + (P_x^2)^T C^{r+1} P_t - x \left((P_x^2(1))^T C^{r+1} P_t \right) - H^T(x) C^{r+1} P_t^\alpha - H^T(x) M P_t^\alpha = 0, \quad (4.4)$$

where $K(x, t) = x \{ y_1(t) - y_0(t) \} + y_0(t) + r(x) - g(x)$.

In discrete form by putting collocation points, Eq(4) in matrix form can be written as:

$$\left((P_x^2)^T - V^{2,1,g(x)} \right) C^{r+1} P_t - H^T C^{r+1} P_t^\alpha = H^T M P_t^\alpha - K, \quad (4.5)$$

where H is the $m \times m$ Haar matrix, $V^{2,1,g(x)} = g(x) I_1^2 H^T = g(x) (P^2(1))^T$, $(g(x) = x)$ is the $m \times m$ fractional integration matrix for boundary value problem, $P_x^\alpha = I_x^\alpha H^T$ and $P_t^\alpha = I_t^\alpha H$ are the $m \times m$ matrices of fractional integration of the Haar function. Also $K = K(x(i), t(i))$, $i = 1, 2, \dots, m$ matrix determined at the collocation points.

By multiplying P^{-1} from right side and $(H^T)^{-1}$ from left side to Eq (4.5), we get:

$$\underbrace{(H^T)^{-1} \left((P^2)^T - V^{2,1,g(x)} \right) C^{r+1}}_A \underbrace{- C^{r+1} P_t^\alpha (P^{-1})}_{-B} = \underbrace{(H^T)^{-1} (H^T M P_t^\alpha - K) (P^{-1})}_C, \quad (4.6)$$

which it is the Sylvester equation ($AX + XB = C$). We solve Eq. (4.6) for C^{r+1} , which is $m \times m$ coefficient matrix, and substituting C^{r+1} in Eqs. (4.4) or (4.2), we get solution $u_{r+1}(x, t)$ at the collocation points. Suppose an initial approximation $u_0(x, t)$, we get a linear fractional partial differential equation in $u_1(x, t)$ by substituting $r = 0$ in Eq. (4.1), where is solved by above procedure. Similarly for $r = 1$ we obtain $u_2(x, t)$ and so on.

4.1. Numerical Examples. In this section, we present Haar wavelet iteration (HWI) method for the numerical solution of the Time Fractional Modified Camassa-Holm and Time Fractional Modified Degasperis-Procesi equations, and the proposed method has been compared with existing method ([16], [17], [18]) to demonstrate its capability.

EXAMPLE 4.1. By putting $b = 2$, equation (1.1) reduces to Time Fractional Modified Camassa-Holm equation.

$$u_t^\alpha - u_{xxt} + 3u^2u_x = 2u_xu_{xx} + uu_{xxx} \quad (4.6)$$

with the initial and boundary conditions:

$$u(x, 0) = -2\operatorname{sech}^2\left(\frac{x}{2}\right), \quad u(0, t) = -2\operatorname{sech}^2(-t), \quad u(1, t) = -2\operatorname{sech}^2\left(\frac{1}{2} - t\right).$$

The corresponding integer order problems $\alpha = 1$ has the exact solution

$$u_{exact} = -2\operatorname{sech}^2\left(\frac{x}{2} - t\right).$$

Suppose $u_0(x, t) = -2\operatorname{sech}^2(\frac{x}{2})$ as an initial approximated and apply the Haar wavelet with iteration technique.

The numerical results for different value resolution (m) and different iteration with $\alpha = 1$ at 5 iterations are shown in Figs 1, 3. Absolute error for different iterations with $\alpha = 1$ in $(x(i), t(i))$ are shown in Fig 2. To make a comparison, the absolute error obtained by the present method has been compared with the Adomian Decomposition Method (ADM) [17] and Variational Iteration Method (VIM) [16], [18] in Table 1.

EXAMPLE 4.2. By putting $b = 3$, equation (1.1) reduce to Time Fractional Degasperis-Procesi equation.

$$u_t^\alpha - u_{xxt} + 4u^2u_x = 3u_xu_{xx} + uu_{xxx} \quad (4.7)$$

with the initial and boundary conditions:

$$\begin{aligned} u(x, 0) &= -\frac{15}{8}\operatorname{sech}^2\left(\frac{x}{2}\right) \\ u(0, t) &= -\frac{15}{8}\operatorname{sech}^2\left(-\frac{5t}{4}\right) \\ u(1, t) &= -\frac{15}{8}\operatorname{sech}^2\left(\frac{1}{2} - \frac{5t}{4}\right). \end{aligned}$$

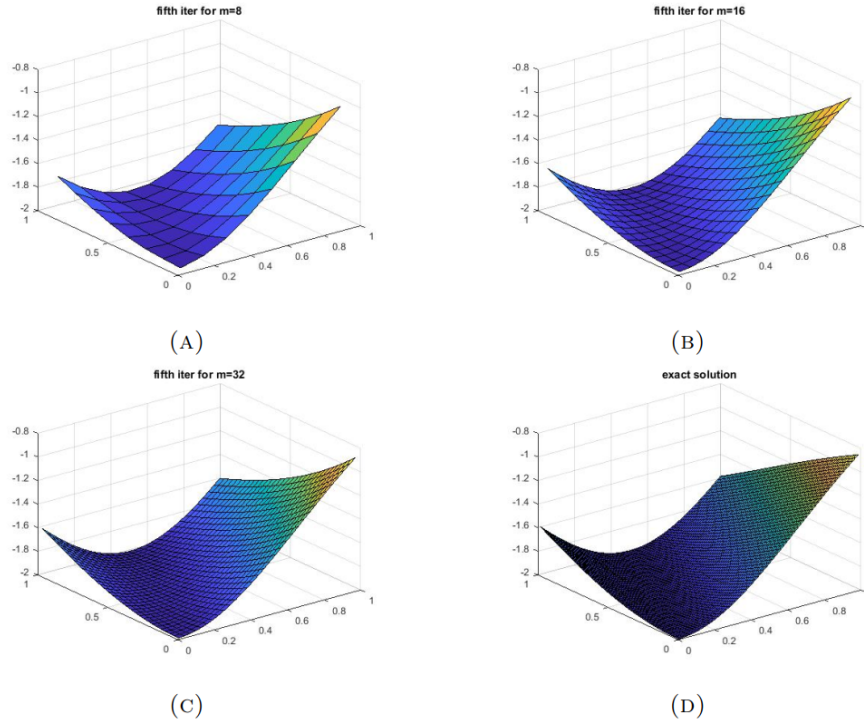


FIGURE 1. Exact solution and Haar wavelet iteration (HWI) solution for different value resolution in Example 4.1, which shows that numerical solution is in very good coincide with exact solution by increasing resolution (m).

The corresponding integer order problems $\alpha = 1$ has exact solution

$$u_{exact} = -\frac{15}{8} \operatorname{sech}^2\left(\frac{x}{2} - \frac{5t}{4}\right).$$

Suppose $u_0(x, t) = -\frac{15}{8} \operatorname{sech}^2(\frac{x}{2})$ as an initial approximated and apply the Haar wavelet iteration technique.

The numerical results include absolute error and approximate solutions for $m = 64$ at 3 iterations are shown in Fig 3. The approximate solutions obtained by the present method has been compared with the Adomian Decomposition Method (ADM) [17] and Variational Iteration Method (VIM) [16], [18] in Table 2 and Table 3 shows the absolute errors of the approximate solutions for different value of α at different points.

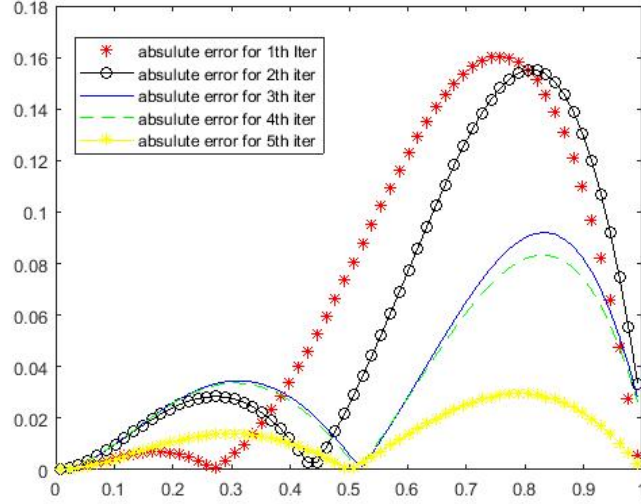


FIGURE 2. Comparison of absolute error for different approximate solutions for $\alpha = 1$, in Example 4.1.

| $(x(i), t(j))$ | $\alpha = 1$ | | | | |
|--------------------------------------|----------------------------|----------------------------|----------------------------|--------------------------------|--------------------------------|
| | $ u_{HWT}^{(1)} - u_{ex} $ | $ u_{HWT}^{(3)} - u_{ex} $ | $ u_{HWT}^{(5)} - u_{ex} $ | $ u_{ADM}^{(2)} - u_{ex} [17]$ | $ u_{VIM}^{(2)} - u_{ex} [18]$ |
| $(\frac{1}{128}, \frac{1}{128})$ | 4.46×10^{-5} | 8.23×10^{-5} | 1.71×10^{-5} | 3.66×10^{-4} | 3.66×10^{-4} |
| $(\frac{15}{128}, \frac{15}{128})$ | 5.31×10^{-3} | 1.26×10^{-2} | 5.22×10^{-3} | 8.17×10^{-2} | 8.17×10^{-2} |
| $(\frac{31}{128}, \frac{31}{128})$ | 3.52×10^{-3} | 3.10×10^{-2} | 1.29×10^{-2} | 3.40×10^{-1} | 3.40×10^{-1} |
| $(\frac{47}{128}, \frac{47}{128})$ | 2.31×10^{-2} | 3.20×10^{-2} | 1.23×10^{-2} | 7.48×10^{-1} | 7.48×10^{-1} |
| $(\frac{63}{128}, \frac{63}{128})$ | 7.34×10^{-2} | 8.28×10^{-3} | 9.84×10^{-4} | 1.263×10^1 | 1.263×10^1 |
| $(\frac{79}{128}, \frac{79}{128})$ | 1.29×10^{-1} | 3.46×10^{-2} | 1.59×10^{-2} | 1.836×10^1 | 1.836×10^1 |
| $(\frac{95}{128}, \frac{95}{128})$ | 1.60×10^{-1} | 7.83×10^{-2} | 2.82×10^{-2} | 2.414×10^1 | 2.414×10^1 |
| $(\frac{111}{128}, \frac{111}{128})$ | 1.30×10^{-1} | 8.94×10^{-2} | 2.59×10^{-2} | 2.822×10^1 | 2.822×10^1 |
| $(\frac{127}{128}, \frac{127}{128})$ | 5.73×10^{-3} | 2.79×10^{-2} | 2.22×10^{-3} | 3.404×10^1 | 3.404×10^1 |

TABLE 1. Absolute error of approximate solution haar wavelet with $\alpha = 1, m = 64$ in Example 4.1, present method solution compared with ADM method [17] and VIM method [16], [18] at various points of x and t .

5. CONCLUSION

In this work, we have applied the combination of Haar wavelet operational matrices method and iteration technique for the solution of time fractional modified Camassa-Holm equation and time fractional modified Degasperis-Procesi

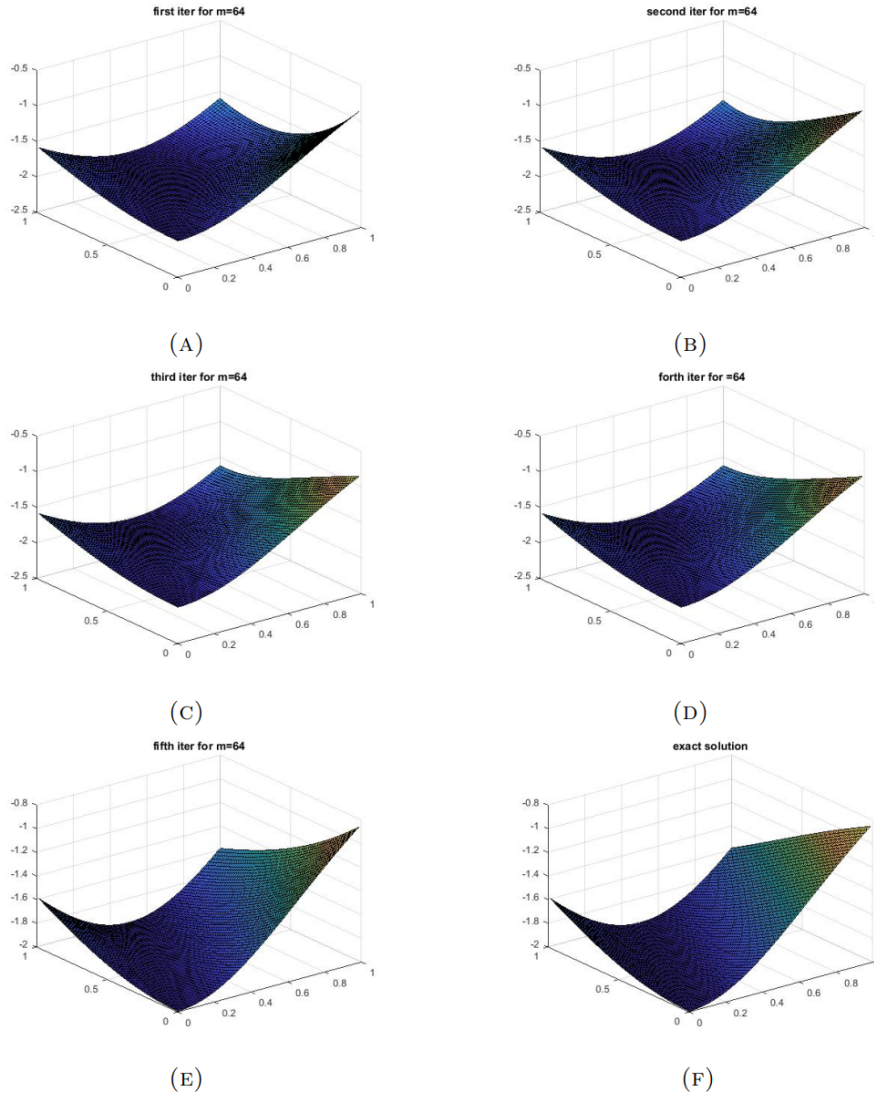


FIGURE 3. Haar wavelet iteration solution for different iterations with $\alpha = 1$ in Example 4.1, which shows that numerical solution is in very good coincide with exact solution by increasing iterations.

equation. We transform nonlinear fractional partial differential equation to the linear equation and Sylvester equation by using iteration technique. The obtained results have been compared with exact solutions as well as with ADM and VIM, which shows that numerical solution are in very good coincide with

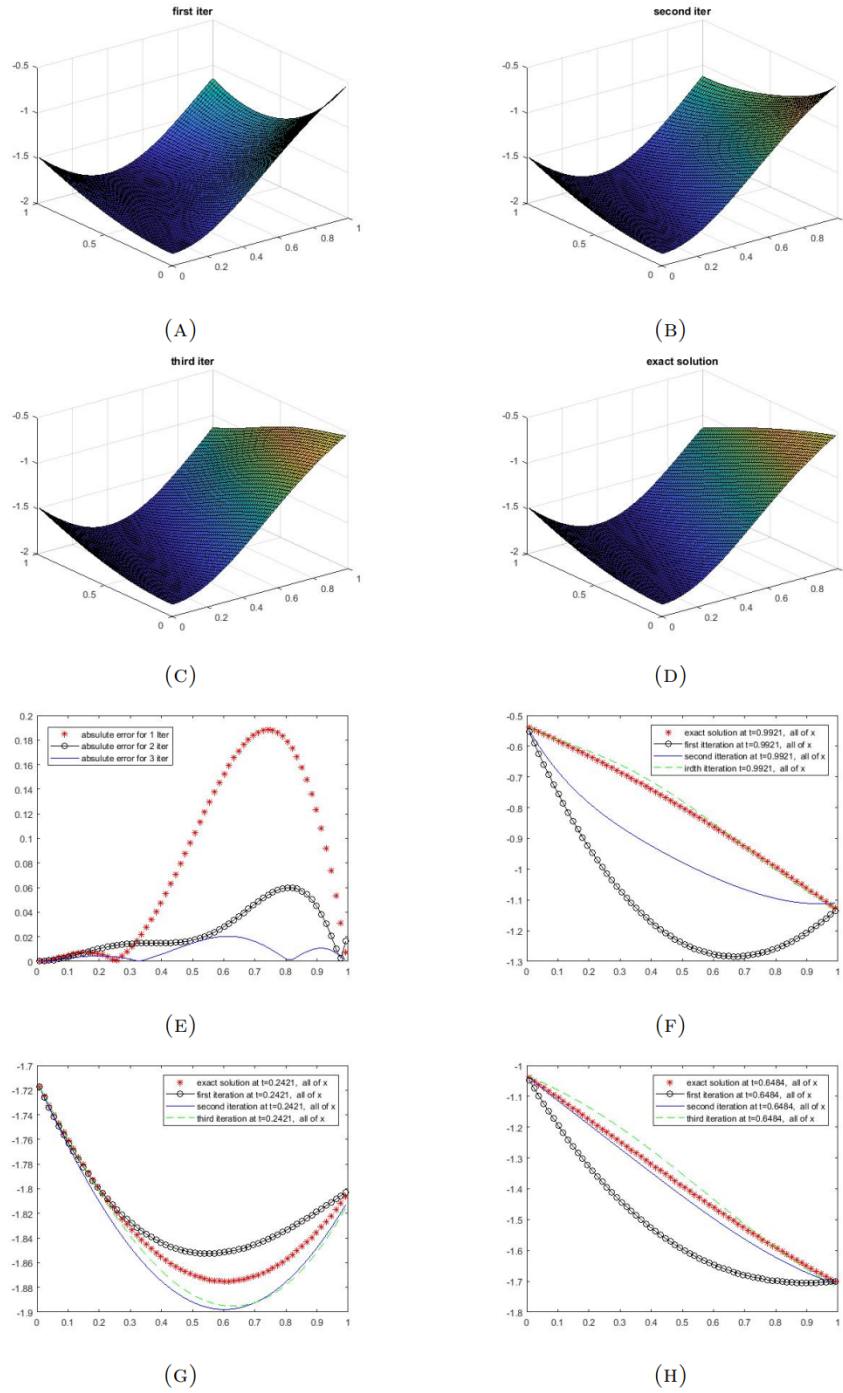


FIGURE 4. Haar wavelet iteration solution for different iterations with $\alpha = 1$, which shows that numerical solution is in very good coincide with exact solution by increasing iterations.

| $(x(i), t(j))$ | $\alpha = 1$ | | | | |
|--------------------------------------|----------------------------|----------------------------|----------------------------|----------------------------|----------------------------|
| | $ u_{HWI}^{(1)} - u_{ex} $ | $ u_{HWI}^{(2)} - u_{ex} $ | $ u_{HWI}^{(3)} - u_{ex} $ | $ u_{ADM}^{(2)} - u_{ex} $ | $ u_{VIM}^{(2)} - u_{ex} $ |
| $(\frac{1}{128}, \frac{1}{128})$ | 5.24×10^{-5} | 2.29×10^{-5} | 2.20×10^{-5} | 1.24×10^{-1} | 1.24×10^{-1} |
| $(\frac{15}{128}, \frac{15}{128})$ | 5.95×10^{-3} | 4.70×10^{-3} | 2.95×10^{-3} | 2.02×10^{-2} | 2.02×10^{-2} |
| $(\frac{31}{128}, \frac{31}{128})$ | 1.62×10^{-3} | 1.25×10^{-2} | 3.90×10^{-3} | 3.10×10^{-1} | 3.10×10^{-1} |
| $(\frac{47}{128}, \frac{47}{128})$ | 3.40×10^{-2} | 1.47×10^{-2} | 2.91×10^{-3} | 8.34×10^{-1} | 8.34×10^{-1} |
| $(\frac{63}{128}, \frac{63}{128})$ | 9.62×10^{-2} | 1.68×10^{-2} | 1.42×10^{-2} | 1.496×10^1 | 1.496×10^1 |
| $(\frac{79}{128}, \frac{79}{128})$ | 1.59×10^{-1} | 3.08×10^{-2} | 2.03×10^{-2} | 2.233×10^1 | 2.233×10^1 |
| $(\frac{95}{128}, \frac{95}{128})$ | 1.88×10^{-1} | 5.39×10^{-2} | 1.11×10^{-2} | 2.979×10^1 | 2.979×10^1 |
| $(\frac{111}{128}, \frac{111}{128})$ | 1.47×10^{-1} | 5.42×10^{-2} | 7.90×10^{-3} | 3.674×10^1 | 3.674×10^1 |
| $(\frac{127}{128}, \frac{127}{128})$ | 7.54×10^{-3} | 1.63×10^{-2} | 1.41×10^{-3} | 4.267×10^1 | 4.267×10^1 |

TABLE 2. absolute error of approximate solution haar wavelet in $\alpha = 1, m = 64$ in Example 4.2, present method solution compared with ADM method [17] and VIM method [16] , [18] at various points of x and t.

| $(x(i), t(j))$ | $ u_{HWI}^{(3)} - u_{ex} $ | $ u_{HWI}^{(3)} - u_{ex} $ | $ u_{HWI}^{(3)} - u_{ex} $ | $ u_{HWI}^{(3)} - u_{ex} $ |
|--------------------------------------|----------------------------|----------------------------|----------------------------|----------------------------|
| | $\alpha = 0.3$ | $\alpha = 0.6$ | $\alpha = 0.9$ | $\alpha = 1$ |
| $(\frac{1}{128}, \frac{1}{128})$ | 4.49×10^{-5} | 4.24×10^{-5} | 3.11×10^{-5} | 2.20×10^{-5} |
| $(\frac{15}{128}, \frac{15}{128})$ | 5.22×10^{-3} | 4.60×10^{-3} | 3.46×10^{-3} | 2.95×10^{-3} |
| $(\frac{31}{128}, \frac{31}{128})$ | 4.82×10^{-3} | 3.89×10^{-3} | 3.62×10^{-3} | 3.90×10^{-3} |
| $(\frac{47}{128}, \frac{47}{128})$ | 1.28×10^{-2} | 1.13×10^{-2} | 6.03×10^{-3} | 2.91×10^{-3} |
| $(\frac{63}{128}, \frac{63}{128})$ | 4.27×10^{-2} | 3.59×10^{-2} | 2.14×10^{-2} | 1.42×10^{-2} |
| $(\frac{79}{128}, \frac{79}{128})$ | 6.83×10^{-2} | 5.53×10^{-2} | 3.13×10^{-2} | 2.03×10^{-2} |
| $(\frac{95}{128}, \frac{95}{128})$ | 6.86×10^{-2} | 5.17×10^{-2} | 2.34×10^{-2} | 1.11×10^{-2} |
| $(\frac{111}{128}, \frac{111}{128})$ | 3.51×10^{-2} | 2.19×10^{-2} | 9.28×10^{-4} | 7.90×10^{-4} |
| $(\frac{127}{128}, \frac{127}{128})$ | 7.46×10^{-3} | 4.22×10^{-3} | 1.86×10^{-4} | 1.41×10^{-4} |

TABLE 3. Absolute error of (HWI) with $\alpha = 1, m = 64$ in Example 4.2. which shows that solutions by present method convergence to the exact solution at $\alpha = 1$, when α approach to 1.

the exact solution by increasing iterations or level of resolution or both. The obtained results demonstrate the accuracy, efficiency, and reliability of the proposed method. Agreement between present numerical results obtained by Haar Wavelet Iteration method with exact solutions appear very satisfactory through illustrative results in Tables and Figures. However, Haar Wavelet Iteration method provides more accurate and better solution in comparison to ADM

and VIM. The present scheme is very simple, effective and appropriate for obtaining numerical solutions of nonlinear partial differential equations.

ACKNOWLEDGMENTS

The authors were supported by *Azarbaijan Shahid Madani University*. The authors express their gratitude to unknown referees for their helpful suggestions which improved the final version of this paper.

REFERENCES

1. J. He, Nonlinear Oscillation with Fractional Derivative and its Applications, *Int. Conf. Vibr. Eng.*, **98**, (1998), 288-291.
2. J. He, Some Applications of Nonlinear Fractional Differential Equations and their Approximations, *Bull. Sci. Technol.*, **15**(2), (1999), 86-90.
3. F. Mainardi, Fractional Calculus: Some Basic Problems in Continuum and Statistical Mechanics, *Fract. Fract. Calculus Contin. Mech.*, (1997), 291-348.
4. R. Panda, M. Dash, Fractional Generalized Splines and Signal Processing, *Signal Proc.*, **86**, (2006), 2340-2350.
5. G. Bohannan, Analog Fractional Order Controller in Temperature and Motor Control Applications, *J. Vibr. Control*, **14**, (2008), 1487-1498.
6. T. Chow, Fractional Dynamics of Interfaces Between Soft-nanoparticles and Rough Substrates, *Phys. Lett., A*, **342**, (2005), 148-155.
7. Y. Li, N. Sun, B. Zheng, Q. Wang, Y. Zhang, Wavelet Operational Matrix Method for Solving the Riccati Differential Equation, *Commun. Nonlinear Sci. Numer. Simul.*, **19**(3), (2014), 483-493.
8. S. Balaji, Legendre Wavelet Operational Matrix Method for Solution of Fractional Order Riccati Differential Equation, *J. Egypt. Math. Soc.*, **23**(2), (2015), 263-270.
9. M. H. Heydari, M. R. Hooshmandasl, F. Mohammadi, Legendre Wavelets Method for Solving Fractional Partial Differential Equations with Dirichlet Boundary Conditions, *Appl. Math. Comput.*, **234**, (2014), 267-276.
10. Y. Li, Solving a Nonlinear Fractional Differential Equation Using Chebyshev Wavelets, *Commun. Nonlinear Sci. Numer. Simul.*, **15**(9), (2010), 2284-2292.
11. Y. Wang, L. Zhu, Solving Nonlinear Volterra Integrodifferential Equations of Fractional Order by Using Euler Wavelet Method, *Adv. Diff. Eq.*, (2017), 17-27.
12. L. Zhu, Y. Wang, Solving Fractional Partial Differential Equations by Using the Second Chebyshev Wavelet Operational Matrix Method, *Nonlinear Dyn.*, **89**, (2017), 1915-1925.
13. F. Zhou, X. Xu, The Third Kind Chebyshev Wavelets Collocation Method for Solving the Time-fractional Convection Diffusion Equations with Variable Coefficient, *Appl. Math. Comput.*, **280**, (2016), 11-29.
14. S. Saha Ray, A. K. Gupta, A Numerical Investigation of Time-fractional Modified Fornberg-Whitham Equation for Analyzing the Behavior of Water Waves, *Appl. Math. Comput.*, **266**, (2016), 135-148.
15. R. E. Bellman, R. E. Kalaba, *Quasilinearization and Nonlinear Boundary Value Problems*, Amer. Elsevier Publishing Company, 1965.
16. M. A. Yousif, B. A. Mahmood, F. H. Easif, A New Analytical Study of Modified Camassa-Holm and Degasperis-Procesi Equations, *Amer. J. Comput. Math.*, **5**, (2015), 267-273.
17. D. D. Ganji, E. M. M. Sadeghi, M. G. Rahmat, Modified Camassa-Holm and Degasperis-Procesi Equations Solved by Adomian's Decomposition Method and Comparison with HPM and Exact Solutions, *Acta Appl Math*, **104**, (2008), 303-311.

18. A. Yildirim, Variational Iteration Method for modified Camassa-Holm and Degasperis-Procesi Equations, *Int. J. Numer. Meth. Biomed. Engng.*, **26**, (2010), 266-272.
19. F. Guo, W. Peng, Blowup Solutions for the Generalized Two-component Camassa-Holm System on the Circle, *Nonlinear Anal.*, **105**, (2014), 120-133.
20. T. Rehman, G. Gambino, S. Roy Choudhury, Smooth and Non-smooth Travelling Wave Solutions of Some Generalized Camassa-Holm Equations, *Commun. Nonlinear Sci. Numer. Simul.*, **19**(6), (2014), 1746-1769.
21. R. Camassa, D. Holm, J. Hyman, A New Integrable Shallow Water Equation, *Adv. Appl. Mech.*, **31**, (1994), 1-33.
22. R. S. Johnson, Camassa-Holm, Korteweg-de Vries and Related Models for Water Waves, *J. Fluid Mech.*, **455**, (2002), 63-82.
23. A. Fokas, B. Fuchssteiner, Symplectic Structures, Their Backlund Transformation and Hereditary Symmetries, *Phys. D.*, **4**, (1981), 47-66.
24. J. Lenells, Conservation Laws of the Camassa-Holm Equation, *J. Phys. A.*, **38**(4), (2005), 869-880.
25. R. Camassa, D. Holm, An Integrable Shallow Water Equation with Peaked Solutions, *Phys. Rev. Lett.*, **71**, (1993), 1661-1664.
26. Y. Zhang, X. J. Yang, An Efficient Analytical Method for Solving Local Fractional Nonlinear PDEs Arising in Mathematical Physics, *Appl. Math. Model.*, **40**, (2016), 1793-1799.
27. J. Ahmad, S. T. Mohyud-Din, H. M. Srivastava, X. Yang, Analytic Solutions of the Helmholtz and Laplace Equations by Using Local Fractional Derivative Operators, *Waves Wavelets Fract. Adv. Anal.*, **1**(1), (2015), 22-26.
28. P. K. Gupta, M. Singh, A. Yildirim, Approximate Analytical Solution of the Time-fractional Camassa-Holm, Modified Camassa-Holm and Degasperis-Procesi Equations by Homotopy Perturbation Method, *Sci. Iranica A*, **23**(1), (2016), 155-165.
29. P. Xiujuan, Sh. Kang, Y. Kwun, Existence and Nonexistence of Solutions for the Generalized Camassa-Holm Equation, *Adv. Diff. Eq.*, **2014**, (2014), 111.
30. Sh. Lai, N. Li, Y. Wu, The Existence of Global Weak Solutions for a Weakly Dissipative Camassa-Holm Equation in $H^1(\mathbb{R})$, *Bound. Value Probl.*, (2013), 13-26.
31. M. K. Jena, K. S. Sahu, Haar Wavelet Operational Matrix Method to Solve Initial Value Problems, *Int. J. Appl. Comput. Math.*, **3**, (2017), 3961-3975.
32. M. A. Iqbal, M. Shakeel, A. Ali, S. T. Mohyud-Din, Improved Wavelets Based Technique for Nonlinear Partial Differential Equations, *Opt. Quant. Electron.*, **49**, (2017), 167.
33. F. K. Yin, W. Y. Han, J. Q. Song, X. Q. Cao, Legendre Wavelets-Picard Iteration Method for Solution of Nonlinear Initial Value Problems, *Int. J. Appl. Phys. Math.*, **3**(2), (2013), 127-131.
34. L. Wang, Y. Ma, Zh. Meng, Haar Wavelet Method for Solving Fractional Partial Differential Equations Numerically, *Appl. Math. Comput.*, **227**, (2014), 66-76.
35. A. Babaaghaie, K. Maleknejad, Numerical Solutions of Nonlinear Two-dimensional Partial Volterra Integro-differential Equations by Haar Wavelet, *J. Comput. Appl. Math.*, **317**, (2017), 643-651.
36. Y. Li, F. Liu, I. W. Turner, T. Li, Time-fractional Diffusion Equation for Signal Smoothing, *Appl. Math. Comput.*, **326**, (2018), 108-116.
37. Y. Li, M. Jiang, F. Liu, Time Fractional Super-diffusion Model and its Application in Peak-preserving Smoothing, *Chemomet. Intel. Labor. Syst.*, **175**, (2018), 13-19.